

## Prediction of brine evaporation rate based on response surface methodology and artificial neural network

Zhiwei Li<sup>a,b,c</sup>, Zhenhai Fu<sup>a,b,\*</sup>, Chengbao Li<sup>a,b</sup>, Dongmei Zhao<sup>a,b</sup>, Yongming Zhang<sup>a,b</sup>, Yanfang Ma<sup>a,b</sup>, Zhihong Zhang<sup>a,b,\*</sup>

<sup>a</sup>Key Laboratory of Comprehensive and Highly Efficient Utilization of Salt Lake Resources, Qinghai Institute of Salt Lake, Chinese Academy of Sciences, Xining 810008, China, emails: fzh@isl.ac.cn (Z. Fu), zhangzh@isl.ac.cn (Z. Zhang), lchb@isl.ac.cn (C. Li), dongmeizh@isl.ac.cn (D. Zhao), yming@isl.ac.cn (Y. Zhang), mayanfang@isl.ac.cn (Y. Ma)

<sup>b</sup>Key Laboratory of Salt Lake Resources Chemistry of Qinghai Province, Xining 810008, China

<sup>c</sup>University of Chinese Academy of Sciences, Beijing 100049, China, email: lizw@isl.ac.cn (Z. Li)

Received 14 March 2021; Accepted 4 June 2021

---

### ABSTRACT

In this study, a Box–Behnken design was carried out to investigate the effects of radiation intensity, environment temperature, relative humidity, brine temperature, wind speed and brine concentration on the brine evaporation rate. The predictive abilities of response surface methodology and artificial neural networks were compared. The results showed that root mean square error for new data by the response surface method and artificial neural network models is 0.265 and 0.125, respectively; whereas the coefficient of determination is 0.773 and 0.940, respectively; and the standard error of prediction is 29.26% and 13.77%, respectively. It indicating that the artificial neural network model has much higher modeling abilities and generalization abilities than the response surface methodology model. Thus, the artificial neural network model is much more stable and accurate to be used in predicting brine evaporation rate in comparison to the response surface methodology model.

*Keywords:* Response surface methodology; Artificial neural network; Brine evaporation rate; Salt Lake

---

### 1. Introduction

Salt Lake is a natural treasure house of inorganic salts. It contains not only common salts such as halite, mirabilite and trona but also precious metal resources such as sylvite, borax, lithium salt, rubidium and cesium that are urgently needed for the development of the national economy, which has excellent development prospects and utilization values [1,2]. The Salt Lake brine resources are abundant in the Qinghai–Tibet Plateau of China. Since the climate characteristics of the plateau lake area are sufficient sunshine, windy and dry, it is suitable to develop and utilize comprehensively Salt Lake brine resources by natural evaporation [3]. However, the brine evaporation rate is an

essential technical parameter for the design, construction and management of salt pans.

As we have known that many factors can affect brine evaporation rate, including external meteorological factors such as radiation intensity, environment temperature, relative humidity and wind speed [4,5] and internal factors such as brine temperature and brine concentration [6]. Generally, the calculation formula of brine evaporation rate is usually expressed by the product of freshwater evaporation rate and conversion coefficient under the same conditions, which are often assumed to be a function of meteorological factors such as environment temperature, wind speed, and relative humidity [7,8]. Unfortunately, these calculation formulas are often subject to geographical restrictions and do not have universal applicability.

---

\* Corresponding authors.

Currently, there are two common modeling methods for the processes affected by multiple factors, namely response surface methodology (RSM) and artificial neural network (ANN). RSM is an efficient modeling tool providing quadratic functions to fit responses in linear or smooth nonlinear processes [9], which is widely used in chemistry, biology and other fields. Compared with a one-factor experimental design, RSM is a time-saving method and also can describe the interactive effect among variables [10–13]. ANN is a modeling method to solve nonlinear and tricky problems by simulating the way that biological brain neurons process information [14]. Compared with RSM, ANN can fit almost all nonlinear processes, but its fitting process is a black-box, and cannot draw specific model expressions to describe the interactive effect among variables [15–17].

Up to now, there are some studies on the freshwater evaporation rate, but less studies on the brine evaporation rate. The purpose of this study is to develop an empirical model, which can accurately predict brine evaporation rate. The influence of main factors on brine evaporation rate was comprehensively considered, the RSM and ANN methodologies were applied for predicting the brine evaporation process, and then modeling abilities and generalization abilities of RSM and ANN models were compared.

## 2. Experimental

### 2.1. Experimental material

The raw brine was taken from Qarhan Salt Lake. The raw brine was diluted with distilled water or condensed by evaporation to different concentrations, and the main chemical composition of brine is shown in Table 1.

### 2.2. Experimental design and procedures

Fig. 1 shows the experimental apparatus for brine evaporation. In this study, a six-factor Box–Behnken design (BBD) was used to design the experiment for constructing models. Brine evaporation rate was chosen as the response variable, while radiation intensity ( $X_1$ ), environment temperature ( $X_2$ ), relative humidity ( $X_3$ ), brine temperature ( $X_4$ ), wind speed ( $X_5$ ) and brine concentration ( $X_6$ ) were chosen as independent variables, respectively. Table 2 summarizes the experimental design levels for BBD, and the experimental design is shown in Table 3.

According to the experimental design in Table 3, different concentrations of brine were prepared first (Table 1), and then put brine into standard evaporating dishes

( $\Phi = 20$  cm). The different experimental conditions including radiation lights, air thermostat, air blower, constant humidity machine and brine thermostat were changed every 5 h.

### 2.3. Analytical methods

The ion concentration of brine was analyzed by using Inductively Coupled Plasma Optical Emission Spectrometer (ICP-OES) (iCAP 6500 DUO, Thermo Fisher Scientific, Waltham, USA) and Ion Chromatography (IC) (ICS-5000+, Thermo Fisher Scientific, Waltham, USA). As shown in Fig. 1,

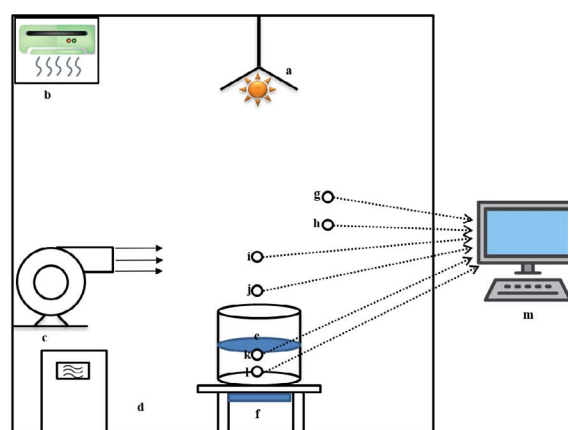


Fig. 1. Schematic diagram of brine evaporator: (a) irradiation light; (b) air thermostat; (c) air blower; (d) constant humidity machine; (e) evaporating dish; (f) brine thermostat; (g) humidity sensor; (h) environment temperature sensor; (i) reference radiometer; (j) anemograph; (k) brine temperature sensor; (l) evaporation sensor; (m) multichannel data collector.

Table 2  
Independent variables and experimental design levels for BBD

Independent variable	Code	Level		
		-1	0	1
Radiation intensity (kW/m <sup>2</sup> )	$X_1$	0	0.5	1
Environment temperature (°C)	$X_2$	15	20	25
Relative humidity (%)	$X_3$	30	40	50
Brine temperature (°C)	$X_4$	20	25	30
Wind speed (m/s)	$X_5$	0	4	8
Brine concentration (mol/kg)	$X_6$	0	5	10

Table 1  
Main chemical composition of brine

	Chemical component (mol/kg)					Total content of main ions (mol/kg)	Density (g/cm <sup>3</sup> )
	Na <sup>+</sup>	K <sup>+</sup>	Mg <sup>2+</sup>	Cl <sup>-</sup>	SO <sub>4</sub> <sup>2-</sup>		
Raw brine	0.408	0.340	2.604	5.766	0.096	9.214	1.264
Experimental brine	0.204	0.169	1.447	3.108	0.064	4.992	1.147
	0.121	0.041	3.259	6.488	0.072	9.981	1.302

Table 3  
Box–Behnken design for brine evaporation experimental

No.	X <sub>1</sub>	X <sub>2</sub>	X <sub>3</sub>	X <sub>4</sub>	X <sub>5</sub>	X <sub>6</sub>	No.	X <sub>1</sub>	X <sub>2</sub>	X <sub>3</sub>	X <sub>4</sub>	X <sub>5</sub>	X <sub>6</sub>
1	0.0	20	40	20	0	5	28	1.0	20	40	30	8	5
2	0.5	20	40	25	4	5	29	1.0	15	40	30	4	5
3	0.0	20	40	30	8	5	30	1.0	20	40	20	0	5
4	0.5	20	40	25	4	5	31	1.0	20	40	20	8	5
5	0.5	20	50	20	4	10	32	0.0	20	30	25	4	10
6	0.5	20	30	30	4	10	33	0.5	25	40	25	8	10
7	0.5	15	40	25	8	10	34	0.5	15	30	25	0	5
8	0.5	15	40	25	8	0	35	1.0	20	40	30	0	5
9	0.0	15	40	30	4	5	36	0.5	20	30	20	4	0
10	0.5	25	40	25	0	10	37	0.0	25	40	20	4	5
11	0.5	25	30	25	0	5	38	0.5	15	30	25	8	5
12	0.5	20	50	30	4	0	39	1.0	15	40	20	4	5
13	0.5	25	40	25	8	0	40	0.5	20	40	25	4	5
14	0.5	25	50	25	8	5	41	0.0	20	40	30	0	5
15	0.5	20	40	25	4	5	42	0.5	20	40	25	4	5
16	0.5	20	50	20	4	0	43	0.5	20	30	30	4	0
17	1.0	25	40	20	4	5	44	0.0	20	40	20	8	5
18	0.5	25	50	25	0	5	45	0.5	20	30	20	4	10
19	0.0	15	40	20	4	5	46	0.0	25	40	30	4	5
20	1.0	20	30	25	4	0	47	1.0	25	40	30	4	5
21	0.5	15	40	25	0	10	48	1.0	20	50	25	4	0
22	1.0	20	50	25	4	10	49	0.5	15	40	25	0	0
23	0.0	20	50	25	4	0	50	0.5	15	50	25	0	5
24	0.5	20	40	25	4	5	51	0.5	20	50	30	4	10
25	0.5	25	30	25	8	5	52	0.0	20	30	25	4	0
26	0.5	25	40	25	0	0	53	0.0	20	50	25	4	10
27	1.0	20	30	25	4	10	54	0.5	15	50	25	8	5

experimental data of radiation intensity, environment temperature, relative humidity, brine temperature, wind speed and brine evaporation were collected by various sensors and multichannel data collectors. Eq. (1) can be used to calculate the brine evaporation rate.

$$Y = \frac{h}{t} \tag{1}$$

where Y (mm/h) is brine evaporation rate, h (mm) is cumulative brine evaporation at evaporation time t (h).

2.4. Response surface methodology

Eq. (2) was used to fit experimental data of brine evaporation rate to construct the RSM model [11,13].

$$Y = b_0 + \sum_{i=1}^n b_i x_i + \sum_{\substack{1 \leq i < j \leq n}} b_{ij} x_i x_j + \sum_{i=1}^n b_{ii} x_i^2 \tag{2}$$

where Y is the corresponding response variable, x<sub>i</sub> and x<sub>j</sub> are actual values of independent variables, b<sub>0</sub> is constant,

b<sub>i</sub> is linear coefficients, b<sub>ij</sub> is interactive coefficients and b<sub>ii</sub> is quadratic coefficients.

2.5. Artificial neural network

A feedforward neural network with a backpropagation (BP) algorithm was applied for modeling the brine evaporation process. In this training process of the BP neural network, the mean square error between the predicted value and experimental value was calculated, and then the error propagated backward through the network as the basis for modifying the weight and bias of each layer. Signal propagated forward, error propagated backward, and weight matrix modified of each layer was repeated until error reaches the expected value [14,15].

The root mean square error (RMSE), coefficient of determination (R<sup>2</sup>) and standard error of prediction (SEP) were calculated by Eqs. (3)–(5) respectively to evaluate the modeling abilities of RSM and ANN models.

$$RMSE = \sqrt{\frac{\sum_{i=1}^n (y_{i,t} - y_{i,p})^2}{n}} \tag{3}$$

$$R^2 = 1 - \frac{\sum_{i=1}^n (y_{i,t} - y_{i,p})^2}{\sum_{i=1}^n (y_{i,t} - \bar{y}_t)^2} \quad (4)$$

$$SEP = \frac{RMSE}{\bar{y}_t} \times 100\% \quad (5)$$

where  $y_{i,t}$  is experimental data,  $y_{i,p}$  is predicted data,  $\bar{y}_t$  is the mean value of experimental data and  $n$  is the number of the experimental data. The smaller RMSE, SEP and the higher  $R^2$ , the more excellent the modeling ability a given model has.

### 2.6. Model validation

The new data which were not used for modeling could be used to evaluating the generalization abilities of RSM and ANN models. Therefore, six additional experiments were carried out based on the numerical range given in Table 1. Table 4 illustrates the experimental data used to validate models.

## 3. Results

### 3.1. Response surface methodology modeling

The data of brine evaporation experimental in Table 5 were used to construct the RSM model. The RSM model [Eq. (6)] was obtained by using Eq. (2) to fit experimental data of brine evaporation rate.

$$\begin{aligned} Y = & 1.5146 + 0.9332X_1 - 0.0800X_2 - 0.0105X_3 - 0.0843X_4 \\ & + 0.0749X_5 + 0.1053X_6 + 0.0028X_1X_2 + 0.0074X_1X_3 \\ & - 0.0533X_1X_4 - 0.0137X_1X_5 + 0.0036X_1X_6 + 0.00015X_2X_3 \\ & + 0.0016X_2X_4 + 0.00048X_2X_5 + 0.00023X_2X_6 + 0.00011X_3X_4 \\ & - 0.00050X_3X_5 + 0.00009X_3X_6 + 0.0020X_4X_5 - 0.0050X_4X_6 \\ & - 0.0071X_5X_6 + 0.5008X_1^2 + 0.00097X_2^2 - 0.00004X_3^2 \\ & + 0.0026X_4^2 - 0.0033X_5^2 - 0.0020X_6^2 \end{aligned} \quad (6)$$

where  $Y$  is brine evaporation rate (mm/h),  $X_1$  is radiation intensity (kW/m<sup>2</sup>),  $X_2$  is environment temperature (°C),  $X_3$  is relative humidity (%),  $X_4$  is brine temperature (°C),  $X_5$  is wind speed (m/s) and  $X_6$  is brine concentration (mol/kg).

Analysis of variance on the RSM model showed that it was significant ( $P < 0.0001$ ) and lack of fit was insignificant ( $P > 0.01$ ), which indicated that it could describe the effect of radiation intensity, environment temperature, relative humidity, brine temperature, wind speed and brine concentration on the brine evaporation rate very well. Accordingly, the data of brine evaporation rate predicted by the RSM model are listed in Table 5.

Eq. (6) shows that brine evaporation rate had a complicated relationship with independent variables, which contained first and second-order polynomial. The effect of two variables on the objective function was analyzed by Eq. (6), while another variable was kept constant [18]. The interactive effects of radiation intensity, environment temperature,

relative humidity, brine temperature, wind speed and brine concentration on brine evaporation rate are given in Fig. 2 when radiation intensity, environment temperature, relative humidity, brine temperature, wind speed and brine concentration were kept constant at 0.5 kW/m<sup>2</sup>, 20°C, 40%, 25°C, 4 m/s and 5 mol/kg, respectively.

Brine evaporation was a multi-factor process, and there was an interaction among the factors. It can be seen directly from Fig. 2 that the interaction among factors was significant except for environment temperature and relative humidity (Fig. 2f). The interaction between radiation intensity and environment temperature (Fig. 2a), radiation intensity and relative humidity (Fig. 2b), radiation intensity and brine temperature (Fig. 2c), radiation intensity and wind speed (Fig. 2d), environment temperature and brine temperature (Fig. 2g), environment temperature and wind speed (Fig. 2h), relative humidity and brine temperature (Fig. 2j), brine temperature and wind speed (Fig. 2m), relative humidity and wind speed (Fig. 2k) were positive, which promoted brine evaporation. On the contrary, the interaction between radiation intensity and brine concentration (Fig. 2e), environment temperature and brine concentration (Fig. 2i), relative humidity and brine concentration (Fig. 2l), brine temperature and brine concentration (Fig. 2n), wind speed and brine concentration (Fig. 2o) were negative, which inhibited brine evaporation.

### 3.2. Artificial neural network modeling

The first step in training a neural network is to design the topology of the ANN model. The number of neurons in the input layer and output layer was determined by the number of inputs and outputs. The most important thing was to determine the number of neurons in the hidden layer. Thus, the RMSE in a different number of neurons were compared to obtain the optimal number of neurons in the hidden layer of the ANN model.

As shown in Fig. 3, the RMSE of ANN first decreased and then increased as the number of neurons increased, which indicated that the ANN model could model brine evaporation rate better when the number of neurons in the hidden layer was seven. Thus, as shown in Fig. 4, the ANN architecture in this study consists of six neurons in the input layer, such as radiation intensity, environment temperature, relative humidity, brine temperature, wind speed and brine concentration, seven neurons in the hidden layer, and one neuron (brine evaporation rate) in the output layer (topology 6-7-1).

Experimental data were normalized to eliminating the difference of values and units among variables [19]. The experimental data of brine evaporation in Table 5 used in constructing the RSM model were selected for training the ANN model. And then, the data of brine evaporation rate predicted by the ANN model were also listed in Table 5.

### 3.3. Comparison of RSM and ANN models

The RMSE,  $R^2$  and SEP for RSM and ANN models were calculated by Eqs. (3)–(5), respectively. As shown in Table 6, RMSE (0.077) and SEP (12.05%) for the RSM model both higher than those (0.073% and 11.37%, respectively) for

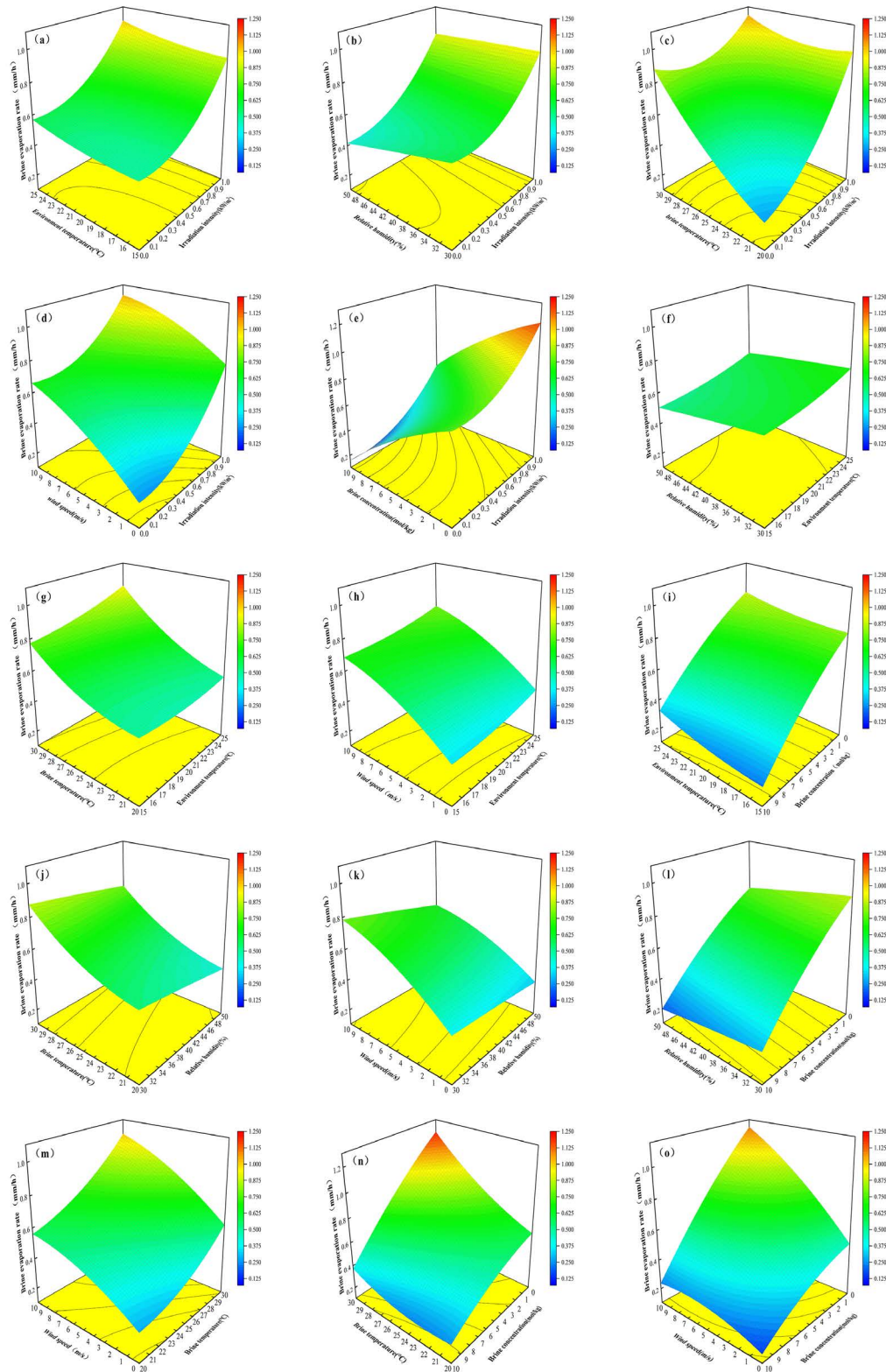


Fig. 2. The 3D response surface plots of interactive effects on brine evaporation rate of: (a) radiation intensity and environment temperature, (b) radiation intensity and relative humidity, (c) radiation intensity and brine temperature, (d) radiation intensity and wind speed, (e) radiation intensity and brine concentration, (f) environment temperature and relative humidity, (g) environment temperature and brine temperature, (h) environment temperature and wind speed, (i) environment temperature and brine concentration, (j) relative humidity and brine temperature, (k) relative humidity and wind speed, (l) relative humidity and brine concentration, (m) brine temperature and wind speed, (n) brine temperature and brine concentration, and (o) wind speed and brine concentration.

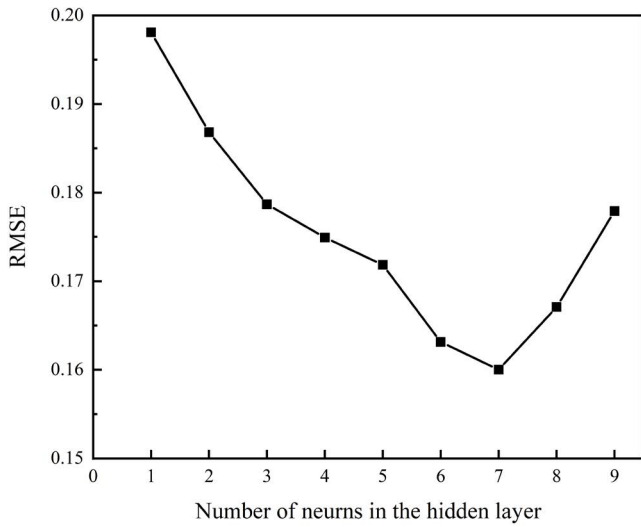


Fig. 3. Effect of number of neurons in the hidden layer on the RMSE.

the ANN model and that the  $R^2$  (0.947) for the ANN model higher than that (0.940) for RSM model. Fig. 5 shows the comparison between the corresponding experimental data and brine evaporation rate predicted by RSM model and ANN model. It was observed that ANN model predictions were much closer to the line of perfect prediction than RSM model predictions. Therefore, these results indicated that the ANN model had a much higher modeling ability than the RSM model.

In addition, the other six sets of experiment data (Table 4), which were not used for modeling, were carried out to check the generalization abilities of the RSM and ANN model. Similarly, RMSE,  $R^2$  and SEP for RSM and ANN models were calculated by Eqs. (3)–(5), respectively. As shown in Table 6, the RMSE for the new data by RSM and ANN models is 0.265 and 0.125, respectively; whereas the  $R^2$  is 0.773 and 0.940, respectively; and the SEP is 29.26% and 13.77%, respectively. The data of brine evaporation rate predicted by RSM and ANN models were plotted against the corresponding experimental data of brine evaporation rate, as shown in Fig. 6. It was

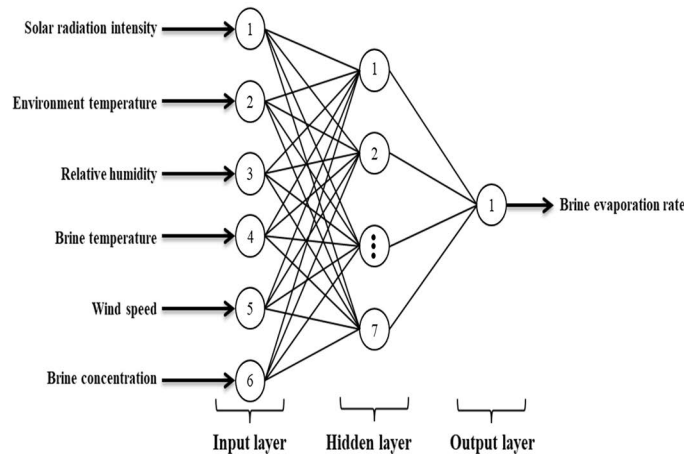


Fig. 4. The topology of artificial neural network.

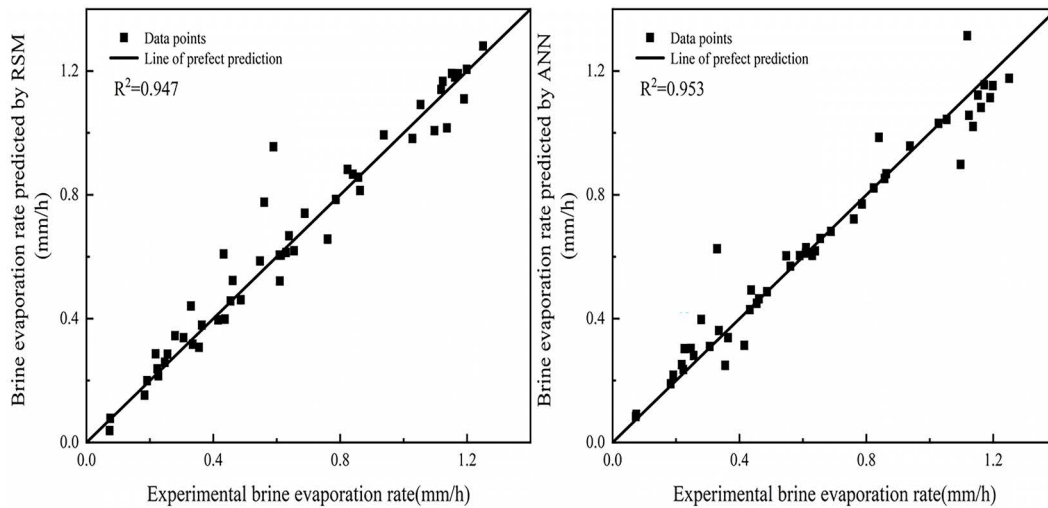


Fig. 5. Brine evaporation rate by RSM and ANN models in model constructing sets.

Table 4  
Experimental data for checking the RSM and ANN models

No.	$X_1$	$X_2$	$X_3$	$X_4$	$X_5$	$X_6$	Brine evaporation rate (mm/h)		
							Actual	RSM predicted	ANN predicted
1	0.25	10	30	15	2	2.5	0.3820	0.4547	0.2887
2	0.25	20	30	25	4	7.5	0.4625	0.4423	0.4770
3	0.25	30	35	35	4	2.5	1.5343	1.9322	1.4553
4	0.75	10	35	15	8	2.5	0.7229	1.0489	0.6536
5	0.75	25	45	30	6	7.5	0.6532	0.8727	0.8564
6	0.75	30	45	35	6	2.5	1.6800	2.0008	1.5008

Table 5  
Experimental data for constructing RSM and ANN models

No.	Brine evaporation rate (mm/h)			No.	Brine evaporation rate (mm/h)		
	Actual	RSM predicted	ANN predicted		Actual	RSM predicted	ANN predicted
1	0.0729	0.0381	0.0832	28	1.1988	1.2053	1.1529
2	0.5475	0.5865	0.6033	29	0.9374	0.9934	0.9575
3	1.1905	1.1099	1.1139	30	0.6094	0.6050	0.6118
4	0.5897	0.9554	0.6039	31	1.0972	1.0073	0.8983
5	0.1913	0.1992	0.2170	32	0.2472	0.2588	0.3037
6	0.3294	0.4407	0.6259	33	0.3062	0.3386	0.3097
7	0.2269	0.2152	0.3029	34	0.4368	0.3982	0.4923
8	1.0532	1.0917	1.0434	35	0.8575	0.8572	0.8529
9	0.8400	0.8668	0.9854	36	0.6882	0.7408	0.6819
10	0.2232	0.2374	0.2352	37	0.2558	0.2849	0.2805
11	0.4543	0.4567	0.4492	38	0.7604	0.6572	0.7220
12	1.1236	1.1667	1.0567	39	0.8626	0.8141	0.8682
13	1.1518	1.1921	1.1223	40	0.6112	0.6050	0.6118
14	0.6544	0.6195	0.6590	41	0.4326	0.6091	0.4289
15	0.5605	0.7761	0.5694	42	0.6294	0.6140	0.6045
16	0.6100	0.5212	0.6294	43	1.2503	1.2807	1.1766
17	1.0279	0.9821	1.0305	44	0.3639	0.3789	0.3383
18	0.4154	0.3957	0.3136	45	0.3352	0.3172	0.3613
19	0.2182	0.2862	0.2512	46	1.1365	1.0159	1.0206
20	1.1719	1.1915	1.1555	47	1.1616	1.1801	1.0820
21	0.1833	0.1524	0.1895	48	1.1182	1.1405	1.3141
22	0.6085	0.6050	0.6118	49	0.4868	0.4609	0.4866
23	0.6136	0.6050	0.6118	50	0.3549	0.3072	0.2490
24	0.6109	0.6050	0.6118	51	0.2795	0.3447	0.3972
25	0.7864	0.7850	0.7705	52	0.8232	0.8819	0.8223
26	0.4613	0.5229	0.4637	53	0.0751	0.0778	0.0906
27	0.6387	0.6678	0.6190	54	0.6115	0.6050	0.6118

observed that ANN model predictions were much closer to the line of perfect prediction than RSM model predictions. The  $R^2$  of the ANN model was higher than that of the RSM model, the RMSE and SEP of the ANN model were lower than those of the RSM model. The above results showed that the generalization ability of the ANN model was superior to that of the RSM model. Compared with the RSM model, which was only suitable for second-order

nonlinear function fitting, the ANN model had higher prediction accuracy because of its strong ability to fit nonlinear functions.

**4. Discussion**

Prior to this paper, scholars have studied the relationship between brine evaporation rate and some factors.

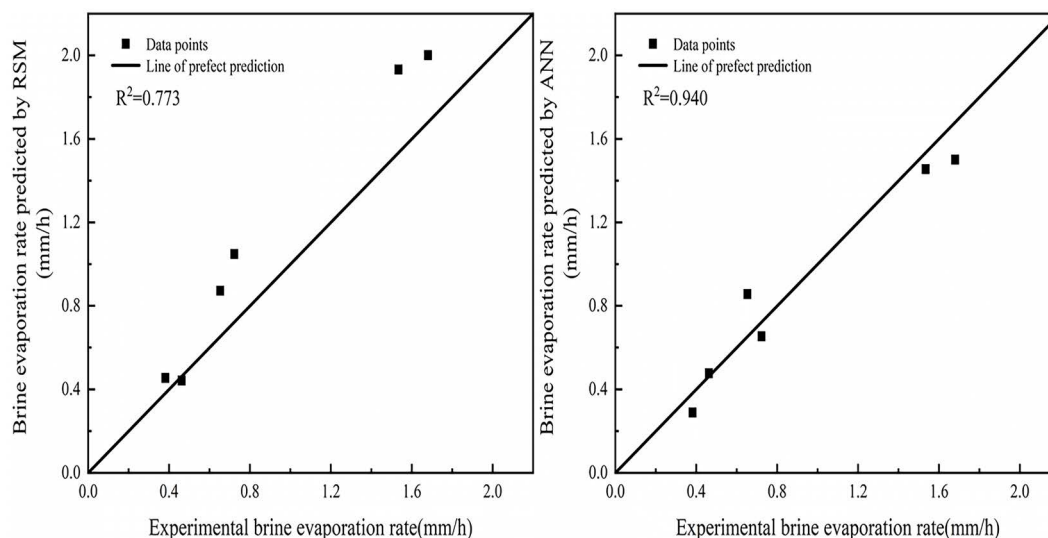


Fig. 6. Brine evaporation rate by RSM and ANN models in model testing sets.

Table 6  
The comparison between RSM and ANN

Parameters	Design data		New data	
	RSM	ANN	RSM	ANN
RMSE	0.077	0.073	0.265	0.125
$R^2$	0.947	0.953	0.773	0.940
SEP	12.05%	11.37%	29.26%	13.77%

Li et al. [20] studied the influence of irradiation intensity and wind speed on the natural evaporation rate, she also found that the evaporation rate increases with the intensity of irradiation and wind speed. Al-Shammiri [21] took into account the effect of salinity on the evaporation rate of brine solutions and established a correlation between various factors and brine evaporation rate. After that, some people used different methods to establish the prediction model of brine evaporation rates such as Salman and Al-Shammiri [6], they built a model to describe the relationship between brine concentration, wind speed, air temperature and evaporation rate. However, by contrast, the advantage of our study is that more factors had been considered to create a predicted model for brine evaporation rate, such as ANN models.

## 5. Conclusion

A Box–Behnken design was carried out to investigate the effects of radiation intensity, environment temperature, relative humidity, brine temperature, wind speed and brine concentration on the brine evaporation process and then modeling abilities and generalization abilities of the RSM model and ANN model were compared. The following conclusions could be drawn.

According to the RSM model, the interaction among factors was significant except for environment temperature and

brine temperature. Either for the prediction of experimental data or new data, the RSME and SEP for the RSM model both higher than those for the ANN model and that the  $R^2$  for ANN model higher than that for the RSM model, indicating that the ANN model had a higher modeling ability and generalization ability than RSM model. Thus, the ANN model is much more stable and accurate to be used in predicting brine evaporation rate in comparison to the RSM model.

The results presented here are of importance to the development and utilization of Salt Lake brine resources, especially the construction and production management of salt pans.

## Acknowledgments

This work was supported by the Qinghai Department of Science and Technology, China (grant numbers 2019-GX-167 and 2019-ZJ-7060); and Innovation Academy for Green Manufacture, Chinese Academy of Sciences (grant number IAGM2020C01).

## References

- [1] P.S. Song, W. Li, B. Sun, Z. Nie, L.Z. Bu, Y.S. Wang, Recent development on comprehensive utilization of Salt Lake resources, *Chin. J. Inorg. Chem.*, 27 (2011) 801–815.
- [2] X.M. Wang, J.D. Miller, F.Q. Cheng, H.G. Cheng, Potash flotation practice for carnallite resources in the Qinghai Province, *Miner. Eng.*, 66–68 (2014) 33–39.
- [3] M.P. Zheng, Y.S. Zhang, X.F. Liu, W. Qi, F.J. Kong, Z. Nie, Progress and prospects of Salt Lake research in China, *Acta Geol. Sin.*, 90 (2016) 1195–1235.
- [4] P. Gamazo, S.A. Bea, M.W. Saaltink, J. Carrera, C. Ayora, Modeling the interaction between evaporation and chemical composition in a natural saline system, *J. Hydrol.*, 401 (2011) 154–164.
- [5] X.K. Wang, Y. Zhou, L. Li, T.C. Gao, N. Tang, Modelling the natural evaporation of the concentrated seawater after desalinated, *Appl. Mech. Mater.*, 713–715 (2015) 2989–2992.
- [6] A. Salman, M.A. Al-Shammiri, New computational intelligence model for predicting evaporation rates for saline water, *Desalination*, 214 (2007) 273–286.

- [7] Y.T. Liu, J.F. Zhang, T. Li, Y.B. Shen, H. Hu, Salt water evaporation test and model correction, *J. Irrig. Drain.*, 37 (2018) 116–120.
- [8] H.J. Liu, S. Cohen, J. Tanny, J.H. Lemcoff, G.H. Huang, Estimation of banana (*Musa* sp.) plant transpiration using a standard 20 cm pan in a greenhouse, *Irrig. Drain. Syst.*, 22 (2008) 311–323.
- [9] R.L. Mason, R.F. Gunst, J.L. Hess, *Statistical Design and Analysis of Experiments: With Applications to Engineering and Science*, Wiley, 2003 doi: 10.1002/0471458503. Available at: <https://onlinelibrary.wiley.com/doi/book/10.1002/0471458503>.
- [10] T. Lau, N. Harbourne, M.J. Oruña-Concha, Optimization of enzyme-assisted extraction of ferulic acid from sweet corn cob by response surface methodology, *J. Sci. Food Agric.*, 100 (2020) 1479–1485.
- [11] L. Peng, Optimization of ethanol fermentation with reducing sugars from *Camellia* (*Camellia oleifera*) seed meal using response surface methodology, *Therm. Sci.*, 22 (2018) 639–647.
- [12] P.A. Sylajakumari, R. Ramakrishnasamy, G. Palaniappan, R. Murugan, Multi-response optimization of end milling parameters for Al-Zn-Mg/SiC Co-continuous composite using response surface methodology, *Mater. Sci.*, 25 (2019) 471–477.
- [13] M. Asadizadeh, H. Masoumi, H. Roshan, A. Hedayat, Coupling taguchi and response surface methodologies for the efficient characterization of jointed rocks' mechanical properties, *Rock Mech. Rock Eng.*, 52 (2019) 4807–4819.
- [14] Y. Lecun, Bengio, G. Hinton, Deep learning, *Nature*, 521 (2015) 436–444.
- [15] Y.C. Wu, J.W. Feng, Development and application of artificial neural network, *Wireless Pers. Commun.*, 102 (2018) 1645–1656.
- [16] M. van Gerven, S. Bohte, Artificial neural networks as models of neural information processing, *Front. Comput. Neurosci.*, 11 (2017) 114.
- [17] A. Erdil, E. Arcaklioglu, The prediction of meteorological variables using artificial neural network, *Neural Comput. Appl.*, 22 (2013) 1677–1683.
- [18] J.Y. Liu, G.F. Zhao, C. Duan, Y.F. Xu, J. Zhao, T. Deng, Effective improvement of activated sludge dewaterability conditioning with seawater and brine, *Chem. Eng. J.*, 168 (2011) 1112–1119.
- [19] N. Asanjarani, M. Bagtash, J. Zolgharnein, A comparison between Box–Behnken design and artificial neural network: modeling of removal of Phenol Red from water solutions by nanocobalt hydroxide, *J. Chemom.*, 34 (2020) e3283, doi: 10.1002/cem.3283.
- [20] L. Li, Y. Zhou, X.K. Wang, T.C. Gao, N. Tang, Study on the relationship between meteorological conditions and brine evaporation rate, *Appl. Mech. Mater.*, 713–715 (2015) 2985–2988.
- [21] M.A. Al-Shammiri, Evaporation rate as a function of water salinity, *Desalination*, 150 (2002) 189–203.